



Contents lists available at ScienceDirect

Chemical Physics Letters

journal homepage: www.elsevier.com/locate/cplett

On the Ewald summation of Gaussian charges for the simulation of metallic surfaces

Todd R. Gingrich*, Mark Wilson

Department of Chemistry, Physical and Theoretical Chemistry Laboratory, University of Oxford, South Parks Road, Oxford OX1 3QZ, UK

ARTICLE INFO

Article history:

Received 16 June 2010

In final form 5 October 2010

Available online 8 October 2010

ABSTRACT

It is shown that standard three- and two-dimensional Ewald summation of point charge electrostatics is naturally extended to Gaussian charge distributions. The Gaussian nature of the charges does not affect the regularisation of the conditionally convergent sums, which are performed with spherical and cylindrical orderings, respectively. A clear connection is made between the summation of Gaussian charges and the summation of the associated point charge system. The application of these sums to a simple classical model of a metal surface is discussed. Calculations on a conducting sphere highlight the importance of the model parameterisation.

© 2010 Elsevier B.V. All rights reserved.

1. Introduction

The construction and application of classical (non-quantum) simulation models (in which the atoms' interactions are represented by relatively simple functions of their positions) remains a crucial field of study. Despite huge advances in quantum methodology, in particular related to the application of density-functional theory (DFT), reliable classical models still afford both greater length- and time-scales to aid the study of fundamental material properties. Furthermore, the ability to effectively tune the underlying interactions (through manipulation of the system parameters controlling the respective contributions to the total potential energy) allows factors which dominate the system properties to be uncovered (an ability which is difficult to achieve within the constraints of a full quantum calculation).

The construction of models with metallic systems presents specific problems due to the polarization of the metal [1–3]. The simulation of the behaviour of ions near metallic surfaces is important if, for example, electrochemical processes are to be effectively modeled [4]. Molecular dynamics simulations of ions near metallic surfaces can be performed with relatively expensive *ab initio* methods [5–7], but to access long time scale dynamics a simpler classical metal model is needed. For macroscopic systems, metal surfaces may be treated with an image charge or Green's function approach [8], but on the microscopic level the atomic structure introduces uncertainty in the exact geometry of the equipotential surface. In general this surface will be corrugated on an atomic scale causing the image charge approach to break down at short range [9].

* Corresponding author.

E-mail addresses: gingrich@berkeley.edu (T.R. Gingrich), mark.wilson@chem.ox.ac.uk (M. Wilson).

Given that the image charge is a mathematical construct to capture the effects of the surface charge distribution, it is natural that the image charge potential can be reproduced at long range by introducing a set of discrete classical surface charges [2]. By treating the surface charge density directly, Finnis et al. demonstrated that even the short-range behaviour of the discrete classical model agrees remarkably well with *ab initio* DFT calculations [10]. More recent work, initiated by Siepmann and Sprik, has furthered this idea by modeling metals as a Gaussian charge on each atomic site, with variable charge magnitudes tuned to make the electric potential at each site equal [11,12]. In essence the model is a rudimentary classical density functional theory with a highly restrictive basis of a single Gaussian per metal atom. This model has allowed relatively long time scales to be accessed, which have enabled fruitful studies of fundamental electrochemistry [13–15].

When models of the type presented by Siepmann and Sprik are treated with periodic boundary conditions, the accurate determination of the (long range) electrostatic interactions is required. One widely used method is the Ewald summation [16] in which the interactions are partitioned into rapidly convergent series, determined in real and reciprocal space, the partition being controlled by a single screening parameter. In order to utilise the potential power of the Gaussian charge models, therefore, the Ewald summation must be adapted to account for these non-point charge distributions. This adaptation has been previously presented for the 2D Ewald summation, but we demonstrate that formula to be slightly erred [12]. The resolution of this error reveals the intuitive fact that an efficient Ewald summation of Gaussian distributions should only differ from the point charge expression in the short-range real space calculation since at sufficiently long-range Gaussians and point charges should become indistinguishable.

It is well known that the Coulomb energy of a periodically replicated system is given by a conditionally convergent infinite series [17]. Such a sum is ill-defined unless the order of summation

is restricted [18]. The convergence factor method of de Leeuw et al. provides a mathematical mechanism for imposing a spherical order of summation [17]. The method isolates the divergences and demonstrates that they vanish in a charge-neutral system. Recent work using a different regularisation method extends these results to charged systems [19]. It is tempting to believe that the Gaussian nature of our charges will not alter the order of summation and the convergence factor results can be borrowed freely, but charge distribution ‘belonging’ to one Gaussian can always be found on either side of a neighbouring site. This complicates the order of summation sufficiently that we chose to explicitly perform the convergence factor calculations. We show that the Ewald summation of Gaussian distributions is in fact a natural extension of the point charge summation. Critically, the two problems are shown to share the same divergent reciprocal space terms such that previous work on the conditional convergence of the point charge system can be freely applied to Gaussian charges.

We proceed to address the 2D Ewald summation of Gaussian charges as presented in the work of Reed et al. [12]. The convergence factor methods are used to reproduce this calculation with a cylindrical order of summation imposed. As with 3D Ewald, it is seen that the differences between Gaussian charges and point charges should be treated entirely in real space. In contrast, earlier work on the subject uses an Ewald screening parameter that depends on the width of the Gaussian charges, so the reciprocal space term is affected by the introduction of Gaussian charges. We show that this is unnecessary since the screening parameter can be adjusted to optimise convergence. Judicious partitioning between the real space and reciprocal space terms reveals that the energy reported by Reed et al. is that of a point charge system with an added on-site Gaussian self-energy. In other words, the energy expression does not reflect the fact that altering the size of the Gaussians also affects the strength of interactions between neighboring sites. We identify and correct the source of this error.

Finally, we reflect upon the selection of the Gaussian width, the only free parameter of the Siepmann/Sprick model [11]. Prior accounts have described fitting this width to continuum limits [11,12]. Clearly these continuum limits must be recovered at macroscopic distances, but we argue that these limits will necessarily be insensitive to the Gaussian size. As a consequence, comparison to the macroscopic behaviour is an improper way to select the Gaussian width. Rather, the parameter should be considered as a crude approximation of the surface atoms’ electronic structure, and should therefore be chosen by fitting to a suitable *ab initio* calculation. The significance of this parameterisation is illustrated by comparing the simple metal model with the analytic image charge solution for a conducting sphere [8].

2. 3D Ewald summation with Gaussian charges

We consider a system of Gaussian charges having spread $(\sqrt{2}\eta)^{-1}$ such that the total charge distribution is

$$\rho(\mathbf{r}) = \sum_{i=1}^n \left(\frac{\eta}{\sqrt{\pi}} \right)^3 q_i \exp(-\eta^2 |\mathbf{r} - \mathbf{r}_i|^2), \quad (1)$$

with the *i*th Gaussian charge centred at \mathbf{r}_i with integrated magnitude q_i . Following the method of de Leeuw et al., the convergence factor $\exp(-s|\mathbf{n}|^2)$ is used to impose a spherical ordering on the sum [17]. We define a uniformly convergent extension of the Coulomb energy, $U_{3D}(s)$ such that the spherically summed Coulomb energy will be returned in the $s \rightarrow 0$ limit:

$$U_{3D}(s) = \frac{\eta^6}{2\pi^3} \sum_{i,j,n} \int_{\mathbb{R}^3} d\mathbf{r}' \int_{\mathbb{R}^3} d\mathbf{r}'' \frac{q_i q_j \exp(-s|\mathbf{n}|^2)}{|\mathbf{r}_{ij} + \mathbf{r}'' - \mathbf{r}' + \mathbf{n}|} \times \exp(-\eta^2 |\mathbf{r}'' - \mathbf{r}_i|^2) \exp(-\eta^2 |\mathbf{r}' - \mathbf{r}_j|^2), \quad (2)$$

where $\mathbf{n} = \mathbf{k}\mathbf{a} + \mathbf{l}\mathbf{b} + \mathbf{m}\mathbf{c}$ for primitive cell vectors \mathbf{a} , \mathbf{b} , \mathbf{c} . Notably the sum includes the $i = j$, $\mathbf{n} = 0$ term that would be excluded from the analogous point charge problem. This on-site Gaussian self-energy reflects the fact that Gaussian charge density on site *i* interacts with the rest of the charge density centred on that same site. As employed previously [12], we make use of the identities

$$|\mathbf{r}_{ij} + \mathbf{r}'' - \mathbf{r}' + \mathbf{n}|^{-1} = \frac{1}{\sqrt{\pi}} \int_0^\infty dt t^{-1/2} \exp(-t|\mathbf{r}_{ij} + \mathbf{r}'' - \mathbf{r}' + \mathbf{n}|^2) \quad (3)$$

and

$$\exp(-\eta^2 |\mathbf{r}|^2) = \left(\frac{1}{2\eta\sqrt{\pi}} \right)^3 \int_{\mathbb{R}^3} d\mathbf{v} \exp\left(-\frac{|\mathbf{v}|^2}{4\eta^2} + i\mathbf{v} \cdot \mathbf{r}\right) \quad (4)$$

to rewrite the energy with integration over dummy variables t , \mathbf{v} , and \mathbf{w} ,

$$U_{3D}(s) = \int_0^\infty dt \int_{\mathbb{R}^3} d\mathbf{r}' \int_{\mathbb{R}^3} d\mathbf{r}'' \int_{\mathbb{R}^3} d\mathbf{v} \int_{\mathbb{R}^3} d\mathbf{w} t^{-1/2} \times \sum_{i,j,n} q_i q_j \exp(-s|\mathbf{n}|^2 - t|\mathbf{r}_{ij} + \mathbf{r}'' - \mathbf{r}' + \mathbf{n}|^2) \times \exp\left(-\frac{|\mathbf{v}|^2}{4\eta^2} + i\mathbf{v} \cdot \mathbf{r}' - \frac{|\mathbf{w}|^2}{4\eta^2} + i\mathbf{w} \cdot \mathbf{r}''\right). \quad (5)$$

Following de Leeuw et al. [17], the algebraic identity,

$$-s|\mathbf{n}|^2 - t|\mathbf{r} + \mathbf{n}|^2 = -(s+t) \left| \mathbf{n} + \frac{t\mathbf{r}}{t+s} \right|^2 - \frac{st|\mathbf{r}|^2}{t+s}, \quad (6)$$

is used with $\mathbf{r} = \mathbf{r}_{ij} + \mathbf{r}'' - \mathbf{r}'$ to give

$$U_{3D}(s) = \frac{1}{2^7 \pi^{13/2}} \int_0^\infty dt \int_{\mathbb{R}^3} d\mathbf{r}' \int_{\mathbb{R}^3} d\mathbf{r}'' \int_{\mathbb{R}^3} d\mathbf{v} \int_{\mathbb{R}^3} d\mathbf{w} \times t^{-1/2} \times \sum_{i,j} q_i q_j \exp\left(-\frac{st|\mathbf{r}_{ij} + \mathbf{r}'' - \mathbf{r}'|^2}{t+s}\right) \times \exp\left(-\frac{|\mathbf{v}|^2 + |\mathbf{w}|^2}{4\eta^2} + i(\mathbf{v} \cdot \mathbf{r}' + \mathbf{w} \cdot \mathbf{r}'')\right) \times \sum_{\mathbf{n}} \exp\left(-(s+t) \left| \mathbf{n} + \frac{t(\mathbf{r}_{ij} + \mathbf{r}'' - \mathbf{r}')}{t+s} \right|^2\right). \quad (7)$$

Jacobi’s imaginary transformation,

$$\sum_{k=-\infty}^{\infty} \exp(-(x+ka)^2 t) = \frac{1}{a} \left(\frac{\pi}{t} \right)^{1/2} \sum_{k=-\infty}^{\infty} \exp\left(-\frac{\pi^2 k^2}{a^2 t} + \frac{i2\pi kx}{a}\right), \quad (8)$$

is applied to Eq. (7), yielding

$$U_{3D}(s) = \frac{1}{2^7 \pi^5 abc} \int_0^\infty dt \int_{\mathbb{R}^3} d\mathbf{r}' \int_{\mathbb{R}^3} d\mathbf{r}'' \int_{\mathbb{R}^3} d\mathbf{v} \int_{\mathbb{R}^3} d\mathbf{w} \times t^{-1/2} (s+t)^{-3/2} \sum_{i,j} q_i q_j \exp\left(-\frac{|\mathbf{v}|^2 + |\mathbf{w}|^2}{4\eta^2}\right) \times \exp\left(-\frac{st|\mathbf{r}_{ij} + \mathbf{r}'' - \mathbf{r}'|^2}{s+t} + i(\mathbf{v} \cdot \mathbf{r}' + \mathbf{w} \cdot \mathbf{r}'')\right) \times \sum_{\mathbf{k}} \exp\left(-\frac{|\mathbf{k}|^2}{4(s+t)} + \frac{it\mathbf{k} \cdot (\mathbf{r}_{ij} + \mathbf{r}'' - \mathbf{r}')}{t+s}\right), \quad (9)$$

where $\mathbf{k} = 2\pi\left(\frac{k}{a}, \frac{l}{b}, \frac{m}{c}\right)$. We now can integrate over \mathbf{r}' and \mathbf{r}'' by changing variables to $\mathbf{r}_+ = \mathbf{r}' + \mathbf{r}''$ and $\mathbf{r}_- = \mathbf{r}'' - \mathbf{r}'$:

$$\begin{aligned}
U_{3D}(s) = & \frac{1}{2^7 \pi^5 abc} \int_0^\infty dt \int_{\mathbb{R}^3} d\mathbf{v} \int_{\mathbb{R}^3} d\mathbf{w} t^{-1/2} (s+t)^{-3/2} \\
& \times \sum_{ij,\mathbf{k}} q_i q_j \exp\left(-\frac{|\mathbf{v}|^2 + |\mathbf{w}|^2}{4\eta^2} - \frac{|\mathbf{k}|^2}{4(s+t)}\right) \\
& \times \int_{\mathbb{R}^3} d\mathbf{r}_- \exp\left(-\frac{st}{t+s} (\mathbf{r}_{ij} + \mathbf{r}_-)^2\right) \\
& \times \int_{\mathbb{R}^3} d\mathbf{r}_+ \exp\left(\frac{2t}{s+t} \mathbf{k} \cdot (\mathbf{r}_{ij} + \mathbf{r}_+)\right) \\
& \times \exp\left[\frac{i}{2} (\mathbf{v} \cdot (\mathbf{r}_+ - \mathbf{r}_-) + \mathbf{w} \cdot (\mathbf{r}_+ + \mathbf{r}_-))\right]. \quad (10)
\end{aligned}$$

Using the standard identity,

$$\int_{\mathbb{R}^3} d\mathbf{r} \exp(i(\mathbf{k} - \mathbf{k}') \cdot \mathbf{r}) = (2\pi)^3 \delta(\mathbf{k} - \mathbf{k}'), \quad (11)$$

we perform the integral over \mathbf{r}_+ to obtain

$$\begin{aligned}
U_{3D}(s) = & \frac{1}{2^4 \pi^2 abc} \int_0^\infty dt \int_{\mathbb{R}^3} d\mathbf{v} \int_{\mathbb{R}^3} d\mathbf{w} (s+t)^{-3/2} \\
& \times t^{-1/2} \sum_{ij,\mathbf{k}} q_i q_j \exp\left(-\frac{|\mathbf{v}|^2 + |\mathbf{w}|^2}{4\eta^2} - \frac{|\mathbf{k}|^2}{4(s+t)}\right) \\
& \times \exp\left(-\frac{i}{2} \mathbf{r}_{ij} \cdot (\mathbf{w} - \mathbf{v})\right) \delta(\mathbf{v} + \mathbf{w}) \\
& \times \int_{\mathbb{R}^3} d\mathbf{r}_- \exp\left(-\frac{st}{t+s} (\mathbf{r}_{ij} + \mathbf{r}_-)^2\right) \\
& \times \exp\left(\frac{i}{2} (\mathbf{w} - \mathbf{v} + \frac{2t}{t+s} \mathbf{k}) \cdot (\mathbf{r}_{ij} + \mathbf{r}_-)\right). \quad (12)
\end{aligned}$$

Changing variables once more to $\mathbf{r} = \mathbf{r}_{ij} + \mathbf{r}_-$ reveals a Gaussian integral over \mathbf{r} . Performing this integration and using the δ -function to eliminate the integral over \mathbf{w} gives

$$\begin{aligned}
U_{3D}(s) = & \frac{1}{2^4 \sqrt{\pi} abc} \int_0^\infty dt \int_{\mathbb{R}^3} d\mathbf{v} t^{-2} s^{-3/2} \sum_{ij} q_i q_j \\
& \times \sum_{\mathbf{k}} \exp\left(-\frac{|\mathbf{k}|^2}{4(s+t)} - \frac{|(s+t)\mathbf{v} - t\mathbf{k}|^2}{4st(s+t)}\right) \\
& \times \exp\left(-\frac{|\mathbf{v}|^2}{2\eta^2} + i\mathbf{r}_{ij} \cdot \mathbf{v}\right). \quad (13)
\end{aligned}$$

The integral over \mathbf{v} is also a Gaussian integral. Integrating one last time leaves

$$\begin{aligned}
U_{3D}(s) = & \frac{\pi \eta^3}{2abc} \int_0^\infty dt t^{-1/2} (2s + (s+t)\eta^2)^{-3/2} \\
& \times \sum_{ij,\mathbf{k}} q_i q_j \exp\left(\frac{-st|\mathbf{r}_{ij}|^2 \eta^2}{2st + (s+t)\eta^2}\right) \\
& \times \exp\left(\frac{i\eta^2 t \mathbf{k} \cdot \mathbf{r}_{ij}}{2st + (s+t)\eta^2} - \frac{|\mathbf{k}|^2 (2t + \eta^2)}{4(2st + (s+t)\eta^2)}\right). \quad (14)
\end{aligned}$$

Inspired by the change of variables used by Reed et al. [12], we let $t' = t\eta^2/(2t + \eta^2)$. After algebraic manipulation, we convert the integral over t into the following integral over t' ,

$$\begin{aligned}
U_{3D}(s) = & \frac{\pi}{2abc} \int_0^{\eta^2/2} dt' t'^{-1/2} (s+t')^{-3/2} \sum_{ij,\mathbf{k}} q_i q_j \\
& \times \exp\left(-\frac{|\mathbf{k}|^2}{4(s+t')} + \frac{it' \mathbf{k} \cdot \mathbf{r}_{ij}}{s+t'} - \frac{st' |\mathbf{r}_{ij}|^2}{s+t'}\right). \quad (15)
\end{aligned}$$

This integral has the same form as that which results from the point charge calculation of de Leeuw et al. [17] except that the upper limit of integration in our Gaussian problem is $\eta^2/2$ instead of infinity. This shows that the summation of Gaussian charges is the natural

extension of the point charge result, which is returned by the $\eta \rightarrow \infty$ limit of Eq. (15). Now consider partitioning the integral over t' at some α^2 , with $\alpha^2 < \eta^2/2$, where α will be the usual Ewald screening parameter. For $t' > \alpha^2$, we can invert the Jacobi transformation, computing that part of the integral in real space,

$$\begin{aligned}
U_{3D}(s) = & \left[\frac{\pi}{2abc} \int_0^{\alpha^2} dt' t'^{-1/2} (s+t')^{-3/2} \sum_{ij,\mathbf{k}} q_i q_j \right. \\
& \times \exp\left(-\frac{|\mathbf{k}|^2}{4(s+t')} + \frac{it' \mathbf{k} \cdot \mathbf{r}_{ij}}{s+t'} - \frac{st' |\mathbf{r}_{ij}|^2}{s+t'}\right) \Big] \\
& + \left[\frac{1}{2} \int_{\alpha^2}^{\eta^2/2} dt' t'^{-1/2} \sum_{ij,\mathbf{n}} q_i q_j \exp(-t|\mathbf{r}_{ij} + \mathbf{n}|^2) \times \exp(-s|\mathbf{n}|^2) \right]. \quad (16)
\end{aligned}$$

The first term is identical to the reciprocal space term of a point charge calculation. It is only in the second term, the real space term, that the Gaussian system differs. The divergences that complicate electrostatics of extended systems all appear in the $\mathbf{k} = 0$ reciprocal space term. Since this term is not affected by the extension to Gaussians, issues of conditional convergence will be identical to the well-studied point charge problem. The regularised Coulomb energy is given by the $s \rightarrow 0$ limit of $U_{3D}(s)$. The $s \rightarrow 0$ limit of the Fourier-space term is provided by de Leeuw et al. [17], while the $s \rightarrow 0$ limit of the real space term is trivial since $\exp(-s|\mathbf{n}|^2)$ can be brought outside the integral. Hence,

$$\begin{aligned}
U_{3D} = & \frac{1}{V} \sum_{\mathbf{k} \neq 0} \frac{2\pi}{k^2} \exp\left(-\frac{k^2}{4\alpha^2}\right) |S(\mathbf{k})|^2 + \frac{1}{2} \int_{\alpha^2}^{\eta^2/2} dt' t'^{-1/2} \\
& \times \sum_{ij,\mathbf{n}} q_i q_j \exp(-t|\mathbf{r}_{ij} + \mathbf{n}|^2) + \frac{\pi}{3V} \sum_{ij} q_i q_j |\mathbf{r}_{ij}|^2, \quad (17)
\end{aligned}$$

where $S(\mathbf{k}) = \sum_{i=1}^n q_i \exp(i\mathbf{k} \cdot \mathbf{r}_i)$ is the structure factor. This final integral can be performed by treating the $i = j$, $\mathbf{n} = 0$ term separately and noting that the integral can be viewed as the difference of an integral from α^2 to infinity and another from $\eta^2/2$ to infinity, each of which can be evaluated as complementary error functions:

$$\begin{aligned}
U_{3D} = & \frac{1}{V} \sum_{\mathbf{k} \neq 0} \frac{2\pi}{k^2} \exp\left(-\frac{k^2}{4\alpha^2}\right) |S(\mathbf{k})|^2 \\
& + \frac{1}{2} \sum_{ij,\mathbf{n}} q_i q_j \frac{\text{erfc}(\alpha|\mathbf{r}_{ij}|) - \text{erfc}\left(\frac{\eta}{\sqrt{2}}|\mathbf{r}_{ij}|\right)}{|\mathbf{r}_{ij}|} \\
& + \left(\frac{\eta}{\sqrt{2\pi}} - \frac{\alpha}{\sqrt{\pi}}\right) \sum_{i=1}^n q_i^2 + \frac{\pi}{3V} \sum_{ij} q_i q_j |\mathbf{r}_{ij}|^2 \\
= & U_{3D}^{pc} - \frac{1}{2} \sum_{ij,\mathbf{n}} \frac{\text{erfc}\left(\frac{\eta}{\sqrt{2}}|\mathbf{r}_{ij}|\right)}{|\mathbf{r}_{ij}|} + \frac{\eta}{\sqrt{2\pi}} \sum_{i=1}^n q_i^2, \quad (18)
\end{aligned}$$

where U_{3D}^{pc} is the 3D Ewald energy for a point charge system. Extension to a mixed system of Gaussians with different widths is a simple matter. The substitution $t' = (\eta_1^2 \eta_2^2 t) / (\eta_1^2 \eta_2^2 + (\eta_1^2 + \eta_2^2)t)$ is used for an interaction between a Gaussian with parameter η_1 and another with η_2 . This includes the interaction with point charges as the $\eta_2 \rightarrow \infty$ limit. The sole effect of these different transformations is to alter the upper limit of integration in Eq. (15), which in turn adjusts the parameter in the complementary error function of Eq. (18).

3. 2D Ewald summation with Gaussian charges

The 2D Ewald summation for Gaussian charges was reported by Reed et al. [12]. Their derivation follows the approach of de Leeuw and Perram in neglecting the potential subtleties of ordering the summation [20]. Grzybowski et al. used convergence factors to

explicitly show that the de Leeuw and Perram result corresponds to a cylindrical sum [21]. In a manner completely analogous to the 3D Ewald discussion of the previous section, the cylindrical sum over Gaussian charges can be viewed as a natural extension of the point charge problem. Integration over the two periodically replicated directions is performed following the steps of Eqs. (10)–(14). The non-periodic z direction does not introduce ambiguities about summation order, so methods used by Reed et al. [12] are utilised to give

$$U_{2D}(s) = \frac{\eta^2}{4ab} \int_0^\infty dt \int_{-\infty}^\infty dt t^{-1} (2st + (s+t)\eta^2)^{-1} \\ \times \sum_{i,j,\mathbf{\kappa}} q_i q_j \exp\left(-\frac{u^2}{4} \left(\frac{1}{t} + \frac{2}{\eta}\right) + iuz_{ij}\right) \\ \times \exp\left(\frac{i\eta^2 t \mathbf{\kappa} \cdot \boldsymbol{\rho}_{ij}}{2st + (s+t)\eta^2} - \frac{|\mathbf{\kappa}|^2 (2t + \eta^2)}{4(2st + (s+t)\eta^2)}\right) \\ \times \exp\left(-\frac{st|\boldsymbol{\rho}_{ij}|^2 \eta^2}{2st + (s+t)\eta^2}\right), \quad (19)$$

where for notational convenience we have written $\boldsymbol{\rho} = (x, y)$ and $\mathbf{\kappa} = 2\pi\left(\frac{k}{a}, \frac{l}{b}\right)$. Finally, the change of variables $t' = \eta^2 t / (2t + \eta^2)$ is applied. Several steps of algebra shows that this transformation maps every term of the integrand onto the form of the associated term that would arise from an Ewald sum over point charges:

$$U_{2D}(s) = \frac{1}{4ab} \int_0^{\eta^2/2} dt' \int_{-\infty}^\infty dt t'^{-1} (s+t')^{-1} \\ \times \sum_{i,j,\mathbf{\kappa}} q_i q_j \exp\left(-\frac{u^2}{4t'} + iuz_{ij}\right) \\ \times \exp\left(-\frac{|\mathbf{\kappa}|^2}{4(s+t')} + \frac{it' \mathbf{\kappa} \cdot \boldsymbol{\rho}_{ij}}{s+t'} - \frac{st' |\boldsymbol{\rho}_{ij}|^2}{s+t'}\right). \quad (20)$$

The only difference between the Gaussian and point charge systems is again the upper limit of t' integration, which is infinity for point charges. This t' integral can be partitioned at α^2 yielding a reciprocal space term which is identical to the point charge problem. Since the divergences are contained in the shared reciprocal space terms, the analysis of Grzybowski et al. of the divergences applies equally well to our Gaussian problem [21]. The real space energy resulting from partitioning the integral is

$$U_{2D}^{real} = \frac{1}{4ab} \int_{\alpha^2}^{\eta^2/2} dt' t'^{-1/2} \sum_{i,j,\mathbf{n}} q_i q_j \times \exp\left(-t'(|\boldsymbol{\rho}_{ij} + \mathbf{n}|^2 + z_{ij}^2)\right), \quad (21)$$

which, assuming a minimum image convention, is the same as the 3D Ewald real-space energy. Using the real space calculation of Eq. (18),

$$U_{2D} = U_{2D}^{pc} - \frac{1}{2} \sum_{i,j,\mathbf{n}} q_i q_j \frac{\operatorname{erfc}\left(\frac{\eta}{\sqrt{2}} |\mathbf{r}_{ij}\right)}{|\mathbf{r}_{ij}|} + \frac{\eta}{\sqrt{2\pi}} \sum_{i=1}^n q_i^2, \quad (22)$$

where U_{2D}^{pc} is the 2D Ewald energy of point charges given by de Leeuw and Perram [20] or by the numerical quadrature approach of Kawata and Mikami [22]. Eq. (22) is precisely the form recently obtained by Vatamanu et al. using a real space decomposition of the pairwise Gaussian interactions [15], but we have shown that this form also correctly compensates for reciprocal space long-range electrostatics.

In practice, a sufficiently large value of the screening parameter α should be chosen to ensure that the minimum image convention for the associated point charge problem is satisfied. Provided $\eta > \sqrt{2}\alpha$, the integral in Eq. (20) can be partitioned and the complementary error function terms shown in Eq. (22) will decay more

rapidly than the $\operatorname{erfc}(\alpha|\mathbf{r}_{ij}|^2)$ terms of the point charge sum. As such, the approximation used by Vatamanu et al. naturally follow from the fact that α was selected to enable the minimum image convention. In a mixed system with both point charges and very broad Gaussian charges it is conceivable that a screening parameter would be selected with $\eta < \sqrt{2}\alpha$. In this scenario the truncation of the Gaussian sum at minimum images does not necessarily follow from the fact that the point charge sums can be treated with minimum images, but such a scenario does not lend itself to a real space calculation. Rather, the integral of Eq. (20) would be computed directly in reciprocal space (the broad Gaussians allowing a rapid Fourier space summation with small truncation error).

It is notable that our result differs from Eq. (A30) in the work of Reed et al. [12]. In their work the upper limit of integration in Eq. (A11) is mistakenly set to infinity instead of $\eta^2/2$. This corresponds to treating the short range electrostatics as point charges rather than Gaussians. In addition, a different partition is applied to the integral over t' . Instead of partitioning at α^2 , the earlier work splits the real space and reciprocal space calculations at β^2 , with $\beta = \eta\alpha(\eta^2 + 2\alpha^2)^{-1/2}$. Despite the different appearance, this does not alter the energy because α and β are both parameters for controlling convergence. The numerical values are chosen to optimise the convergence, but provided the sums are fully converged, the energy is independent of this partition. Furthermore, since the reciprocal space term is identical for point charges as for Gaussians, the numerically optimal screening parameter will be the same for both systems.

4. Application to a simple test system

The simulation of metallic systems presents the challenge of compensating for induced surface charge. Image charge or Green's functions approaches are generally useful, but on a microscopic level the details of the atomic structure make it difficult to specify the corrugated geometry of the equipotential surface. To overcome this challenge, Siepmann and Sprik [11] presented a model which directly calculates the surface charge density by expressing it as a superposition of Gaussian charges centred on each atom of the metal. The Gaussian charge magnitudes are determined to equate the electric potential experienced at the centre of each metal site, thereby imposing the metallic constraint of continuum electrostatics on a discrete lattice [11]. This removes the need to explicitly describe the shape of the equipotential surface. Instead, these atomic effects are controlled by the size of the Gaussian charges, the single parameter of the Siepmann/Sprik model. We applied Ewald summation of Gaussian charges to re-examine the importance of this parameter, η , revealing that short range interactions between a point charge and the metal appear particularly sensitive to the parameterisation.

To highlight this sensitivity we chose to examine the textbook example of an interaction between a conducting sphere and a point charge. A grounded conducting sphere of radius 7.94 Å was modelled with 2000 Gaussian charges of the form given by Eq. (1) centred along a golden section spiral so as to achieve approximately equal spacing between sites [23]. A version of Eq. (18) including interactions with the single point charge and with the so-called tin foil boundary conditions [24] were applied to describe the Coulomb energy. Periodic images were positioned far away from each other by using a cubic box with side lengths 42.33 Å, and the Ewald screening parameter was set to $\alpha = 0.132 \text{ \AA}^{-1}$. Calculations were performed on the periodic system since this form of the Coulomb energy will be required for future work. To confirm that neighbouring replicas do not bias the results, the calculations were reproduced with a wholly real space calculation of the finite system. A single point charge with magnitude e was placed inside the sphere,

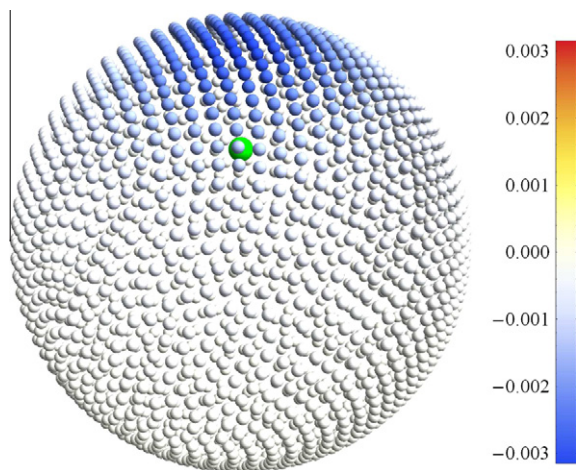


Figure 1. Induced charge distribution on a 7.94 Å radius sphere composed of 2000 Gaussian sites ($\eta = 4.7 \text{ \AA}^{-1}$) with a unit point charge (shown as a larger circle) positioned 3.97 Å from the centre of the sphere. The colour coded charge distribution is given in units of the point charge. The Gaussian sites are shown as circles with radius η^{-1} . (For interpretation of the references in color in this figure legend, the reader is referred to the web version of this article.)

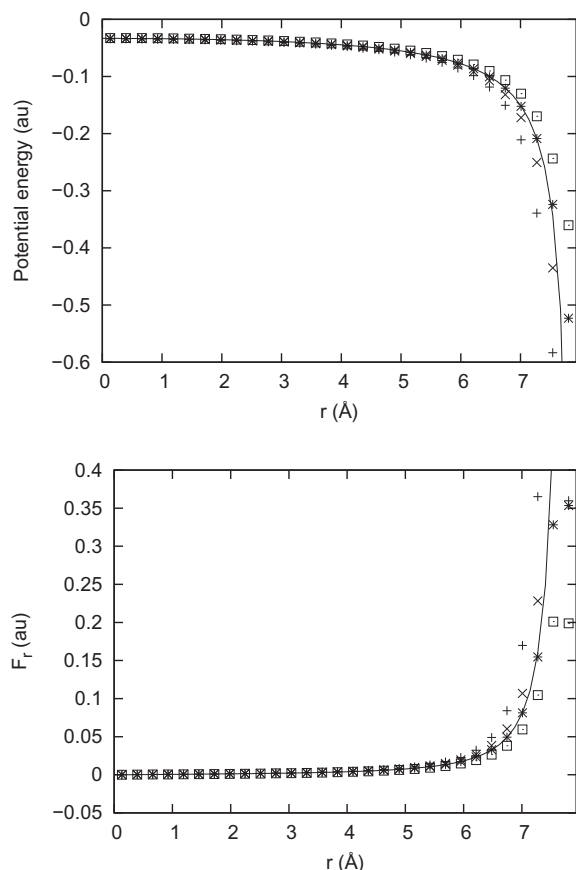


Figure 2. Potential energy of (top), and radial force acting upon (bottom), a point charge a distance r from the centre of a 7.94 Å radius conductive sphere. The calculation is performed with the equipotential constraint enforced over 2000 sites of the sphere. The analytic image sphere result is given by the solid line. Computational results are shown for $\eta = 1.89 \text{ \AA}^{-1}$ (+), 3.78 \AA^{-1} (×), 5.67 \AA^{-1} (*), and 7.56 \AA^{-1} (□).

and the charge distribution on the conducting sphere was computed using the conjugate gradient method to minimize the Coulomb energy [12]. Figure 1 shows the induced charge distribu-

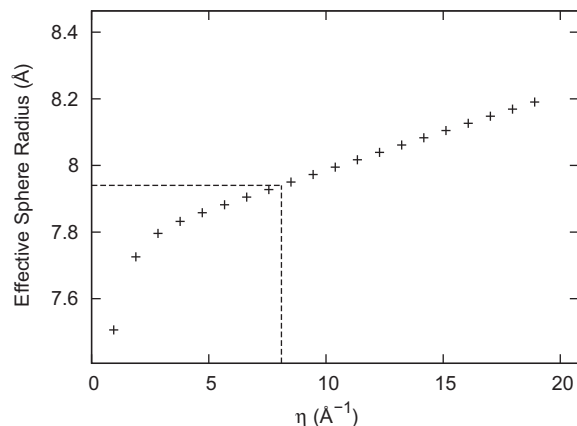


Figure 3. An effective image sphere radius, calculated by fitting the asymptotic ($r < R/3$) behaviour observed in Figure 2 to the continuum image charge energy given by Eq. (23). The effective sphere radius differs from the physical radius of 7.94 Å except when $\eta \approx 8 \text{ \AA}^{-1}$ (as indicated by the dashed lines). Agreement at $\eta \approx 8 \text{ \AA}^{-1}$ does not imply that this is the optimal value of the parameter η (see text).

tion for a particular point charge position and choice of η . In this case $\eta = 4.7 \text{ \AA}^{-1}$ and the point charge is placed 3.97 Å from the centre of the sphere.

The point charge was moved radially inside the sphere and the charge distribution on the sphere was calculated for several values of η . Since the average distance between sites was 0.63 Å, η was varied between 0.95 and 9.45 Å^{-1} , corresponding to Gaussian spreads between 0.75 and 0.08 Å. In Figure 2 the computational results are compared with the standard analytic image charge solution for the energy of, and the radial force acting upon a point charge in, a conducting sphere [8],

$$U = -\frac{q_{\text{point}}^2 R}{2(R^2 - r^2)}, \quad F_r = -\frac{q_{\text{point}}^2 Rr}{(R^2 - r^2)^2}, \quad (23)$$

where r is the displacement of the point charge from the centre of the sphere and R is the radius of the sphere. The force exerted by the metal on a point charge at long range converges to the continuum result for all computed values of η . At short range, the choice of η exerts considerable influence because it constrains the induced charge density to be bound more or less tightly to the atomic sites.

An effective sphere radius can be defined by fitting the long-range portion ($r < R/3$) of Figure 2 to the continuum energy expression, Eq. (23). Figure 3 summarises the η -dependence of this effective radius, which equals the physical radius when $\eta \approx 8 \text{ \AA}^{-1}$. Equality of the physical and the effective long-range image planes implies that the model conductor will behave precisely like a spherical conductor at long range. This equivalence motivated Siepmann and Sprik's initial parameterisation, which has followed through to subsequent works [12–15]. However, we note that our model conductor is not intended to be a smooth sphere on the atomic scale. Indeed, the corrugated equipotential is considered a desirable aspect of the model, and so the metal's capacitance can be expected to deviate slightly from the capacitance of a perfect sphere. As a result, it is not necessary for η to be tuned to a value that forces perfect agreement with the results of a perfect continuum sphere. What is essential is that the metal appears to behave like a metal at distances for which the discrete nature of the surface becomes insignificant. It is clear from Figure 2 that the force on a long range point charge is insensitive to η . Figure 3 expresses this insensitivity in a different form. The differences between effective and geometric image sphere radii are so small that they are insignificant to a long-range point charge. A notable exception occurs as η is increased towards the infinite limit, at which point the

Gaussians become point charges with infinite self-energies. As η increases, the effective sphere radius also increases without bound. Therefore one must pass to longer and longer range before forces will asymptotically approach the continuum limit, with $\eta = \infty$ failing to reproduce long-range electrostatics at any finite range. For this reason, the numerical analysis was restricted to modest values of η , but this restriction can be rationalised on physical grounds. A metal's electronic density is delocalized on the atomic scale, which should be interpreted as the intersite distance, so large η can be disregarded as inappropriate representations of delocalized charge.

We conclude that a point charge far from our model electrode experiences a force which essentially acts like the ideal smooth conductor at long range for a wide range of sufficiently delocalized Gaussian spread. However, Figure 2 makes it clear that short-range forces depend strongly on η , suggesting that the parameterisation should be determined by the short-range behavior. In describing the charge density as a superposition of Gaussians on each site, it is implicitly assumed that a Gaussian is a reasonable approximation of the local electronic structure and that the dominant excitations correspond to redistribution of delocalized charge along a conductor. If the model is to be used to generate short-range interactions with a metal surface, this assumption should be verified and η must be fitted to experimental or computational studies of the metal's electronic structure. We envision determining an optimal value of η from DFT calculations in much the same way that the polarizabilities were recently fitted for an ionic liquid in contact with a metallic surface [25].

5. Conclusions

The aim of this work was to shed light on the method of Ewald summation applied to Gaussian charges. We have shown that the extension from point charges to Gaussian charges is natural, even with the inclusion of a spherical convergence factor. As a result, the extensive analysis of divergences within periodically replicated point charge systems may be applied when the charges are Gaussian in nature. The extension was shown to remain valid for Ewald summation with two periodically replicated directions. Finally, we

have considered the use of these Gaussian charge systems for simulation of metals. Unlike the Ewald screening parameter, α , we note that the Gaussian charge parameter, η , is physically significant. As η controls the representation of the metal's electronic structure, we suggest that future work will need to more carefully parameterise the value in order to generate accurate short-range forces.

Acknowledgments

The authors thank Professor Paul Madden FRS FRSE and Professor Michiel Sprik for encouraging discussions. T.R.G. acknowledges the financial support of the Rhodes Trust.

References

- [1] J. Bardeen, Phys. Rev. 58 (1940) 727.
- [2] M. Finnis, Acta. Metall. Mater. 40 (1992) S25.
- [3] N. Lang, W. Kohn, Phys. Rev. B 7 (1973) 3541.
- [4] E. Wernersson, R. Kjellander, J. Chem. Phys. 125 (2006) 144701.
- [5] D.L. Price, J.W. Halley, J. Chem. Phys. 102 (1995) 6603.
- [6] A. Klesing, D. Labrenz, R. van Santen, J. Chem. Soc., Faraday Trans. 94 (1998) 3229.
- [7] A. Lozovoi, A. Alavi, J. Kohanoff, R. Lynden-Bell, J. Chem. Phys. 115 (2001) 1661.
- [8] J.D. Jackson, Classical Electrodynamics, third edn., John Wiley & Sons Inc., 1999.
- [9] R. Jones, P. Jennings, O. Jepsen, Phys. Rev. B 29 (1984) 6474.
- [10] M. Finnis, R. Kaschner, C. Kruse, J. Furthmüller, M. Scheffler, J. Phys. Condens. Matter 7 (1995) 2001.
- [11] J.I. Siepmann, M. Sprik, J. Chem. Phys. 102 (1995) 511.
- [12] S.K. Reed, O.J. Lanning, P.A. Madden, J. Chem. Phys. 126 (2007) 084704.
- [13] S. Reed, P. Madden, A. Papadopoulos, J. Chem. Phys. 128 (2008) 124701.
- [14] A. Willard, S. Reed, P. Madden, D. Chandler, Faraday Discuss. 141 (2009) 423.
- [15] J. Vatamanu, O. Borodin, G. Smith, Phys. Chem. Chem. Phys. 12 (2010) 170.
- [16] P.P. Ewald, Ann. Phys. 64 (1921) 253.
- [17] S.W. de Leeuw, J.W. Perram, E.R. Smith, Proc. R. Soc. Lond., Ser. A 373 (1980) 27.
- [18] W. Rudin, Principles of Mathematical Analysis, third edn., McGraw-Hill, 1976.
- [19] H.D. Herce, A.E. Garcia, T. Darden, J. Chem. Phys. 126 (2007) 124106.
- [20] S.W. de Leeuw, J.W. Perram, Mol. Phys. 37 (1979) 1313.
- [21] A. Grzybowski, E. Gwóźdź, A. Bródka, Phys. Rev. B 61 (2000) 6706.
- [22] M. Kawata, M. Mikami, Chem. Phys. Lett. 340 (2001).
- [23] E. Saff, A. Kuijlaars, Math. Intell. 19 (1997) 5.
- [24] M. Neumann, Mol. Phys. 50 (1983) 841.
- [25] M. Pounds, S. Tazi, M. Salanne, P. Madden, J. Phys. Condens. Matter 21 (2009).